# Water Coning, Water, and $CO_2$ Injection in Heavy-Oil Fractured Reservoirs

**Joachim Moortgat,** The Ohio State University, and **Abbas Firoozabadi,** Reservoir Engineering Research Institute

## Summary

In this work, we investigate challenges related to the recovery of heavy viscous oil from reservoirs with a dense network of fractures and vugs but with a tight matrix. Gravitational drainage of oil from the tight matrix through water injection is ineffective because of the high oil viscosity and density. To further complicate matters, we consider a strong underlying aquifer, and there is considerable risk of water coning around producing wellbores caused by the low water viscosity. To model potential recovery strategies, we carry out simulations with our higher-order finite-element (FE) compositional multiphase-flow reservoir simulator. Discrete fractures are represented through the crossflow equilibrium (CFE) approach. Phase behavior and phase-split computations are modeled with the cubic-plus-association equation of state (EOS). Fickian diffusion, facilitating species exchange between gas in fractures and matrix oil, is modeled through chemical potential gradients. First, we validate our simulator by modeling a set of laboratory experiments in which water is injected in a fractured stack saturated with oil. The experiments investigate the effects of capillary pressure and injection rates on oil recovery, and show that, at low injection rates, capillary imbibition of water from the fractures into the matrix blocks is extremely efficient. Simulations with our 3D discrete-fracture model show excellent agreement with the experimental results without parameter adjustments. Next, we consider the detrimental effect of water coning when oil is produced without injection by carrying out a parameter study investigating the impacts of different (1) water–oil mobility ratios, (2) matrix and fracture wettabilities, (3) matrix permeabilities, (4) domain sizes, (5) production rates, (6) well types and placement, and (7) a local viscosity-reduction treatment around producing wellbores. We find that the only approach to partially mitigate coning is to produce at low rates from perforated (and potentially multilateral) horizontal wells. As an alternative production strategy, we then model carbon dioxide ($CO_2$) injection in two and three dimensions, and compare to results from a commercial dual-porosity simulator. $CO_2$ has a high solubility in this oil, and dissolution leads to volume swelling and a large reduction in oil viscosity. In combination with the much higher density difference between the phases, the latter improves gravitational drainage. We find that a significant amount of matrix oil can be produced in addition to oil from fractures and vugs, and with a lower risk of water coning.

## Introduction

When oil with a viscosity significantly higher than that of water is produced from densely fractured reservoirs with an underlying aquifer, such as the carbonate reservoirs in some offshore fields, there is an inherent risk of water coning (Beveridge et al. 1970; Pérez-Martínez et al. 2012). Coning is a viscous flow instability caused by the high adverse mobility ratio between oil and the water in the aquifer (Saffman and Taylor 1958; Tan and Homsy 1986; Jiang and Butler 1998). Oil production creates pressure gradients throughout the reservoir that drive flow. At the water–oil contact, two-phase flow favors water because of its higher mobility. A dense network of connected fractures provides a pathway for water to the producers, which can result in early breakthrough and poor oil recovery. A similar coning problem can occur from a low-viscosity gas cap (Singhal 1996). The severity of the coning, as for viscous fingering, depends on (1) the production rate (Abass and Bass 1988; Giger 1989), which determines the pressure gradients; (2) the viscosity contrast between the two phases (water–oil or gas–oil); and (3) the density difference, which determines the stabilizing gravitational drainage of denser water (Muskat and Wyckoff 1935). For fractured reservoirs, the propagation of the coning front depends further on the petrophysical properties, such as the fracture density, fracture and matrix permeabilities, fracture–matrix porosity partitioning, and the wettability of the rock, which determines capillary imbibition of water from the fractures into the matrix. Finally, the impact of coning on oil recovery is affected by production strategy (in addition to rate). The time of breakthrough is determined by the distance of the wells from the water–oil (or gas–oil) contact, and pressure gradients are influenced by the type of wells—that is, vertical or (multilateral Verga et al. 2005) horizontal wells. Operational constraints also determine the amount of water production that can be handled by surface facilities. Most offshore oil fields, in Mexico for instance, currently lack such facilities (Pérez-Martínez et al. 2012). Significant water production caused by coning requires wells to be shut in prematurely. Below a certain critical production rate (Schols 1972), viscous forces are balanced by gravity, and coning can be prevented, but for densely fractured reservoirs, the subcritical production rates may be too low to be economically viable.

Because of the potentially disastrous impact of water coning on oil production, there is considerable interest in better modeling capabilities of coning in fractured media, which is considered one of the most-challenging problems in reservoir engineering. Early theoretical (Muskat and Wyckoff 1935; Chaney et al. 1956; Schols 1972; Giger 1989) as well as numerical studies (Beveridge et al. 1970; Letkeman and Ridings 1970; Settari and Aziz 1974) have been carried out in the distant past. More recent studies of water coning in fractured media have relied on the dual-porosity and dual-permeability models (Warren and Root 1963; Firoozabadi and Thomas 1990; Pérez-Martínez et al. 2012). It is well-known, however, that dual-porosity models, although computationally efficient, compromise in the representation of the relevant physics, especially for complicated multiphase problems. Fractures and matrix blocks are modeled on two dual grids, and all interactions between the fractures and the matrix have to be described by semiempirical transfer functions, which may not be rigorous. Gravitational reinfiltration, capillary effects, phase behavior in compositional multiphase flow, Fickian diffusion, and general configurations of fractures are difficult to reconcile with the dual-porosity framework (though modifications have been proposed to improve on several of these limitations).

In this work, we study coning with a discrete fracture model that explicitly takes into account all convective, capillary, gravitational, and diffusive fluxes between the fractures and the matrix. To the best of our knowledge, coning has not been studied in the context of discrete-fracture models before, and doing so provides new insights into the process that may not have been captured by earlier studies.

In our model, discrete fractures are combined with a small neighborhood of the matrix blocks into larger computational elements. The assumption is that the fluid in the fractures instantaneously equilibrates (mixes) with the fluid immediately next to it in the matrix caused by a high transverse matrix–fracture flux (which does not need to be explicitly calculated). This assumption is



Original SPE manuscript received for review 31 May 2016. Paper (SPE 183648) peer approved 8 July 2016.

referred to as the CFE approach, and the computational elements that contain both the fracture and some matrix fluid are CFE elements. The flux across the edges between two CFE grid cells properly integrates over the fracture aperture and width of the matrix slice, taking into account different relative permeabilities in the fracture and matrix. For example, the matrix part of the CFE may have a high residual oil saturation (ROS), whereas the fracture part may not have residual oil. In the direction orthogonal to the fractures, the flux between a CFE element and a matrix element is equivalent to that between two matrix elements. This approach was first applied to single-phase (Hoteit and Firoozabadi 2005) and two-phase (Hoteit and Firoozabadi 2006) compressible and compositional flow without capillarity in 2D fractured domains, and more recently to three-phase compositional flow in 3D domains with capillarity (Moortgat and Firoozabadi 2013a, 2013b, 2013c). Alternative discrete-fracture models have been proposed for black oil (Geiger et al. 2009) and immiscible incompressible flow (Hoteit and Firoozabadi 2008).

In this work, we first demonstrate the accuracy and reliability of our discrete-fracture model by simulating a set of experiments in which water was injected in a fractured stack saturated with oil (Pooladi-Darvish and Firoozabadi 2000). Capillary imbibition between the fractures and the water-wet matrix is studied as a function of injection rate. The same experiment was modeled before using a control-volume finite-difference method (Monteagudo and Firoozabadi 2007).

Our studies of water coning and $CO_2$ injection consider vuggy reservoirs with a triple porosity of matrix, vugs, and fractures. In our representation of such domains, we divide the triple porosity into CFE elements that contain both the fractures and the connected vugs, and matrix elements that contain the tight matrix and unconnected vugs. A large fraction of the oil may reside in the fractures and vugs, which makes the CFE approach particularly suitable. Similar conditions were investigated before in a dual-porosity framework (Pérez-Martínez et al. 2012).

To model compressible and compositional multiphase flow, we use a higher-order discontinuous Galerkin (DG) method for the transport equations, which updates the molar density of each fluid component. The flow equations are solved by a mixed hybrid finite-element (MHFE) method, which simultaneously solves for globally continuous velocity and pressure fields, both to the same order accuracy. An accurate velocity field in heterogeneous and fractured domains is the main strength of the MHFE approach. More generally, the combination of the DG and MHFE higher-order FE methods is a considerable improvement over lowest-order finite-difference and finite-volume methods, particularly for fractured reservoirs. A detailed description of these methods and comparisons to other approaches are given in our earlier work (Moortgat and Firoozabadi 2010, 2013a, 2013b, 2013c; Moortgat et al. 2012).

After demonstrating that early water coning is likely to occur in densely fractured carbonate reservoirs with an underlying aquifer, we investigate $CO_2$ injection as an alternative production strategy for the same reservoir conditions, but with an even denser fracture network. During $CO_2$ injection, the fractures provide a large interaction surface through which Fickian diffusion can occur, driving species exchange between the fractures and the matrix, thereby delaying breakthrough of injected gas. In addition, mixing of $CO_2$ with the dense viscous oil in this reservoir results in advantageous phase behavior. $CO_2$ has a 75% solubility in this oil, which can lead to 40% swelling of the oil volume (expelling it from the matrix), and a 25-fold reduction in the oil viscosity, which improves gravitational drainage of oil from the matrix into the fractures. The modeling of multicomponent multiphase Fickian diffusion is challenging, particularly in fractured domains, where the conventional description in terms of compositional gradients fails. We resolved these issues in a recent work (Moortgat and Firoozabadi 2013a) by considering gradients in chemical potential as the driving force. The importance of Fickian diffusion when gas is injected in fractured reservoirs is another example where most reservoir simulators have severe limitations. We show that an improper treatment of diffusion can result in significantly underestimating the efficient oil recovery from $CO_2$ injection. In addition, we compare our results to a commercial dual-porosity reservoir simulator that uses our model for Fickian diffusion.

The paper is organized as follows. First, we model a set of experiments (Pooladi-Darvish and Firoozabadi 2000) in which water is injected at different rates into a stack of chalk blocks divided by a number of discrete fractures, and then we investigate the importance of capillary imbibition into the water-wet matrix. The modeling of this complicated experiment demonstrates the reliability of our discrete-fracture model in accurately reproducing experimental data. We then proceed to study the risks of water coning when dense and viscous oil is produced from a fractured reservoir that has an underlying aquifer. The third study considers the alternative of $CO_2$ injection, in which Fickian diffusion and favorable phase behavior lead to considerably higher oil recovery without risk of coning. We end with concluding remarks.

## Experiment and Modeling of Water Injection Into a Fractured Stack

Pooladi-Darvish and Firoozabadi (2000) performed a set of experiments in which water was injected into the bottom of a fractured stack of oil-saturated Kansas chalk blocks. Initially, the stack was saturated with $n$-$C_{10}$ at atmospheric pressure and room temperature (59°F). At these conditions, the "oil" density is 0.8 g/cm$^3$, and the viscosity is 0.94 cp, whereas the water density and viscosity are 0.95 g/cm$^3$ and 1 cp, respectively (note that, in this experiment, the flow is viscously stable). The relative permeability and capillary pressure curves in the fracture and matrix are given in **Fig. 1** and are chosen the same as in an earlier analysis (Monteagudo and Firoozabadi 2007). Details are provided in the figure caption. Of particular importance in the discussion that follows is the ROS of 35%.

The dimensions of the stack are $19 \times 19 \times 122$ cm$^3$, with vertical fractures on all four sides as well as at $x = 6.35$ cm and $x = 12.7$ cm. Horizontal fractures are at the top and bottom as well as at $z = 30.5$ cm, $z = 61$ cm, and $z = 91.5$ cm. These fractures separate 12 matrix blocks with a porosity of 30% and permeability of 2.5 md. The fractures have apertures in the range of 150–200 μm. For our numerical modeling, we assume 2-mm crossflow elements with $1.4 \times 10^6$ md permeability (using the cubic law in terms of the aperture), and we consider three levels of grid refinement: Grid 1 ($13 \times 7 \times 41$), Grid 2 ($13 \times 13 \times 79$), and Grid 3 ($7 \times 6 \times 29$). The configuration of the fractures and chalk slabs are illustrated for Grid 2 in **Fig. 2,** with four boundary fractures omitted for visualization.

In the experiment, water is injected from the bottom at four constant injection rates of 0.26, 0.78, 1.95, and 3.85 pore volumes (PV) per day with constant pressure production from the top. Fig. 2 shows the water saturation at 40% PV injected (PVI) for all four rates simulated on the finest Grid 2. As expected, we find that propagation of water through the fractures is delayed by capillary imbibition into the matrix blocks, which is most effective for the lowest rates.

The measured and simulated (on all three grids) oil-recovery factors for all injection rates are given in **Fig. 3.** The ultimate oil recoveries at 2 PVI, from lowest to highest injection rates, are 67.5, 66.8, 64, and 63.3%, showing a maximum incremental recovery of 6.6% because of the efficiency of capillary imbibition at lower injection rates. At the lowest injection rate, we have essentially piston-like displacement of the nonresidual matrix oil: The front propagates at the same rate in the matrix and the fracture, resulting in the sharp cutoff in recovery at the time of water breakthrough. Note that the oil-recovery factor is higher than $1 - S_{row} = 65\%$ because we include the 2.5% of oil initially in the fractures. We emphasize that such high oil recovery from fractured reservoirs caused by imbibition does not only occur at the laboratory scale, but also in densely fractured field-scale reservoirs (Moortgat and Firoozabadi 2013b, 2013c).

We can accurately simulate this complex problem of two-phase flow with capillarity in a 3D fractured domain with our CFE discrete-fracture model, and the results have essentially converged even on the coarsest grid. In our simulations, no

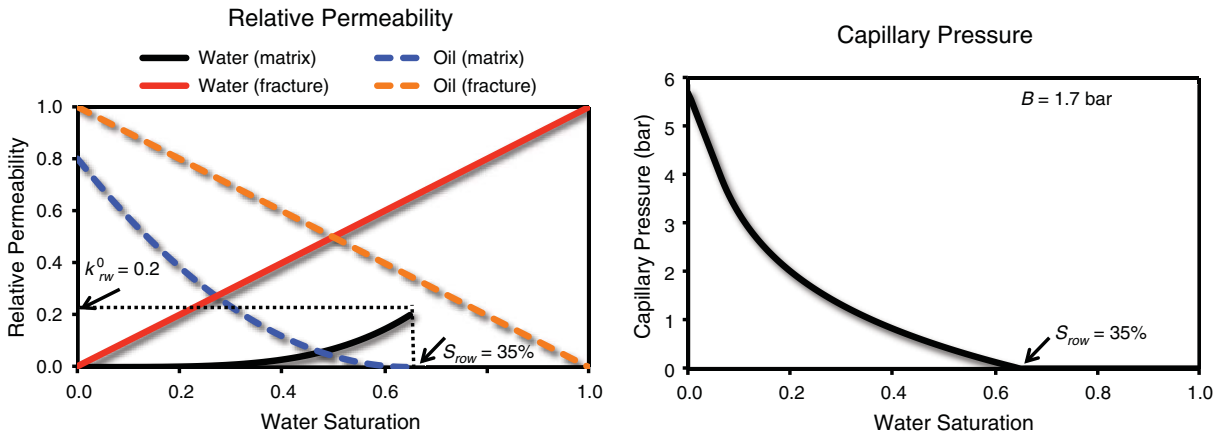


**Fig. 1—Relative permeabilities are linear with unit endpoints in the fracture. In the matrix, the water relative permeability has an exponent of 4 and endpoint of 0.2, whereas the oil relative permeability is quadratic with endpoint 0.8. The ROS is $S_{row} = 35\%$. The water–oil capillary pressure in the matrix is $p_c(\text{bar}) = -B\ln S_{w,\text{eff}}$ with $B = 1.7$ bar, and is linearly extrapolated for effective water saturations [$S_{w,\text{eff}} = S_w/(1-S_{row})$] below 0.1 for numerical stability. Because the capillary pressure scales with $\sqrt{\phi/K}$, the capillary pressure in the fractures is effectively zero (because the fracture permeability is $6 \times 10^5$ times the matrix permeability).**

parameters were adjusted to match the experimental results. The central processing unit (CPU) times for the simulations with our compositional model were 3 hours on Grid 1, 16 hours on Grid 2, and 30 minutes on Grid 3. This compares favorably to modeling of the same experiment on a 1,800-element grid with a control-volume finite-difference method for an immiscible formulation (Monteagudo and Firoozabadi 2007), which required 27 hours of CPU time (on a Pentium PC 2.66 GHz, vs. a 2.8 GHz Intel i7 core used in this work). If we had used an immiscible formulation, our CPU efficiency would have been even higher. Moreover, our CFE model becomes more efficient for large-scale domains in which we can allow for wider crossflow elements than the 2-mm widths used in this example.

This comparison to experimental data gives us confidence in the modeling of larger scale problems considered in the next examples. The more-general conclusion from this example is that waterflooding can be highly effective for densely fractured water-wet reservoirs caused by capillary imbibition.

## Water Coning in Fractured Offshore Heavy-Oil Reservoir With Underlying Aquifer

We study the effect of coning when oil is produced without injection from a heavy-oil reservoir with a strong underlying aquifer. As discussed in the Introduction, we consider reservoirs with a complicated triple porosity consisting of tight matrix, a large number of connected and unconnected vugs, and a dense network of fractures. However, although the effective reservoir permeability is known, the details of the fracture network are not. With this uncertainty, there are several ways that we can set up our simulations: We can have a large number of fractures with a small aperture, or a smaller number of fractures with a wider aperture. The latter allows coarser grids and more-efficient computations. Fracture spacing and matrix block size will affect the fracture–matrix interactions, which will be considered in the examples.

**Reservoir Description and Simulation Setup.** The flux through the fractures depends (numerically) on the fracture aperture times

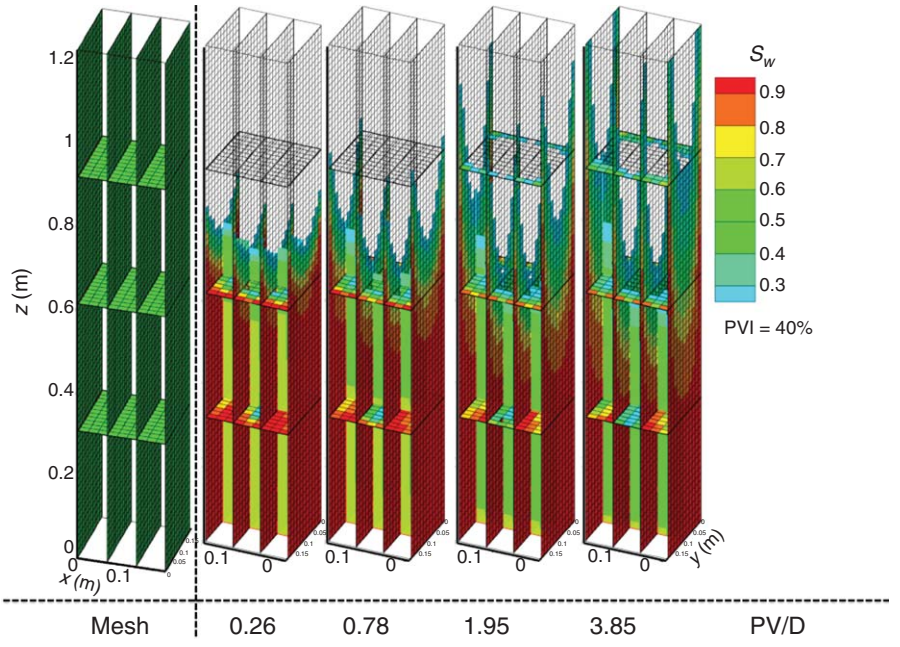


**Fig. 2—Configuration of the fractured stack in the Pooladi-Darvish and Firoozabadi (2000) experiments, and Grid 2 ($13 \times 13 \times 79$ elements) used for the modeling (left). The fractures at the top, bottom, front, and back are omitted for a clearer visualization. Water saturation (right four panels) at 40% PV of water injection at 0.26, 0.78, 1.95, and 3.85 PV/D, projected on slices through four vertical and three horizontal fractures.**

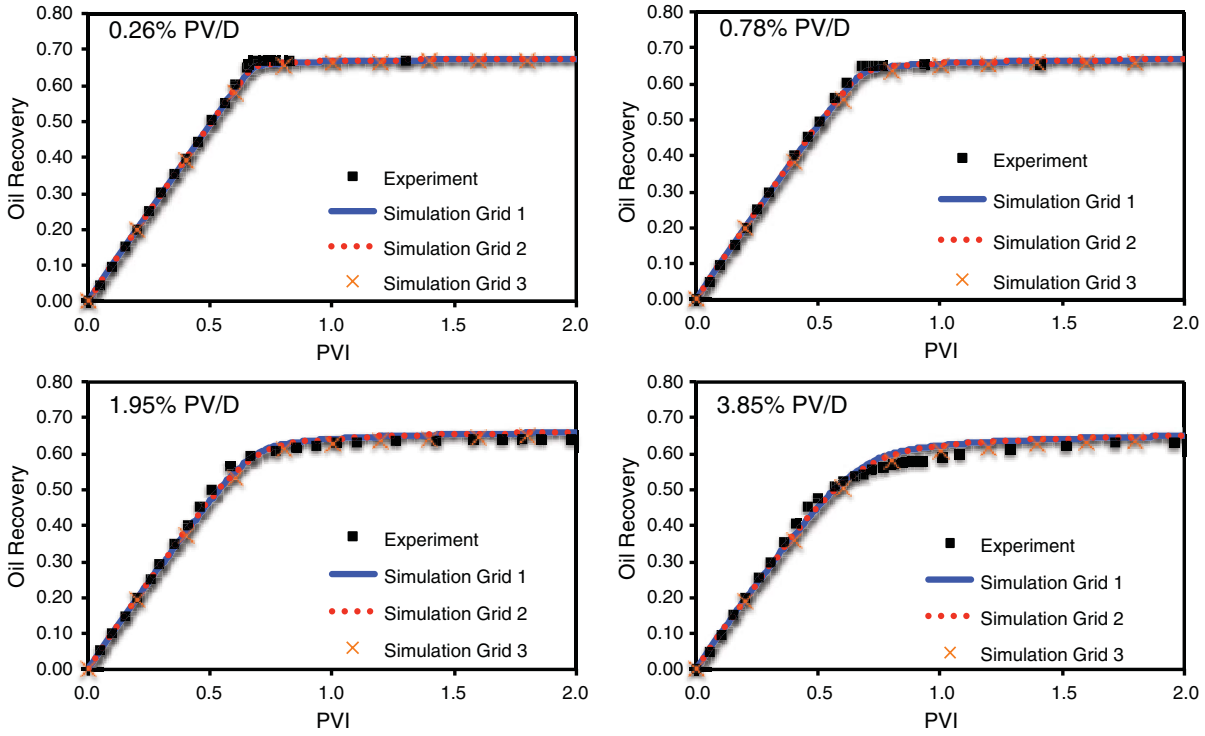


**Fig. 3—Oil recovery for water injection at 0.26, 0.78, 1.95, and 3.85 PV/D. Experimental data points and simulations results on Grid 1 (13 × 7 × 41), Grid 2 (13 × 13 × 79), and Grid 3 (7 × 6 × 29).**

the fracture permeability: We can decrease one and increase the other and obtain similar results. Instead of using the cubic law between fracture aperture and permeability, we choose the fracture aperture, fracture spacing, and fracture permeability to agree with a measured effective permeability of approximately 1 darcy (on the basis of well testing) and a given fraction of oil in the fractures and the vugs. Specifically, as a base case, we consider $4 \times 4\,m^2$ matrix blocks, surrounded by 4-cm fractures with a permeability of 100 darcies, and 40-cm-wide CFE elements that represent both the fractures and connected vugs. The matrix (and unconnected vugs) blocks have a porosity of 8% and a permeability of 1 md. With this configuration, the effective permeability in each direction is 1 darcy, the fraction of oil in the fractures is 20%, and the fraction of oil in the fractures plus the connected vugs is 33%. This high fraction of oil in fractures and vugs in certain offshore Mexican oil reservoirs is what makes them potentially attractive for hydrocarbon production. As we will see next, very-little matrix oil can be recovered through depletion. The recovery from water injection is also known to be low, because of mixed-wetting conditions.

For most of our simulations, we assume a 180-m oil column with a large underlying aquifer. In the horizontal directions, we will investigate the importance of domain size by considering 52- and 400-m dimensions in these directions, and in the vertical direction, we will consider two examples with a 380-m-thick reservoir. Because the Darcy flow in the matrix blocks is slow at best, those are discretized by single grid cells to speed up the computations [discretizing the matrix blocks with multiple grid cells is more critical when capillarity is important, to resolve saturation gradients (as in the previous example) or to resolve compositional gradients that drive Fickian diffusion (as in the final example)]. The aquifer is modeled by the grid cells in the bottom 20 m of the mesh. These elements are given a porosity of 100, which results in a similar pressure gradient at the water–oil contact as having very large (or many) grid cells with the same porosity as elsewhere. By having a large PV of slightly compressible water in the domain, we prevent the pressure from dropping unrealistically fast while we produce from the reservoir without injection. Specifically, the maximum pressure drop in the simulations for 10 years of production is kept below 2,500 psi. By comparison, assigning the same aquifer grid cells a porosity of 1.0 results in a pressure drop to atmospheric pressure in less than 2 years. Physically, this setup corresponds to having either a thick or wide aquifer with enough volume to absorb some of the pressure response in relatively small subdomains.

As an example of coning in fractured heavy-oil reservoirs, we use a fluid from a previous study in which the critical component properties are provided (Moortgat and Firoozabadi 2013a). The initial composition and computed Fickian diffusion coefficients (used in the last example) are summarized in **Table 1.** We consider a reservoir temperature of 226°F and initial bottomhole pressure of 5,459 psi. For the coning study, phase behavior is not pronounced because the pressures remain well above the bubble-point pressure (740 psi), and there is no gas injection. Water will flow through the domain because of the coning process, but this involves immiscible two-phase flow. The main parameters that affect immiscible flow are the oil density, which is $0.976\,g/cm^3$, and a viscosity of 121 cp. This viscosity is taken from field data, but in one of the examples, we also consider the degree of coning for lower oil viscosities of 80, 40, and 12 cp. Oil (and gas) viscosities are computed from the Lohrenz et al. (1964) approach and can be adjusted by tuning the critical volume of the residue ($C_{12+}$). We consider a water density of $0.971\,g/cm^3$ and a constant viscosity of 0.26 cp. The high oil- to water-viscosity ratio (a factor 471) is the critical parameter that causes the coning phenomenon.

In the matrix and the vugs, we assume a quadratic relative permeability for oil and a cubic relation for water with a 50% ROS to water. The endpoint relative permeabilities are 1.0 for oil and 0.3 for water. In the fractures, we assume linear relative permeabilities with unit endpoints as the base case. We also investigate the sensitivity to different relations for both matrix and fracture relative permeabilities. In all but one of the examples, we consider an oil-wet formation and neglect capillarity. In one example, we show that capillary imbibition for a water-wet rock does not significantly change the results.

As a base case, we produce at a constant rate of 5% PV per year without injection. This rate is defined in terms of the total hydrocarbon (HC) PV in the fractures, vugs, and matrix, and

| $z_i$ | | $CO_2$ | $N_2$ | $H_2S$ | $C_1$ | $C_{2-3}$ | $C_{4-6}$ | $C_{7-11}$ |
|---|---|---|---|---|---|---|---|---|
| 5.96 | $CO_2$ | 82.24 | –1.77 | –2.05 | –3.08 | –1.42 | –0.51 | 0.30 |
| 1.80 | $N_2$ | –0.29 | 93.43 | –0.49 | –0.88 | –0.32 | –0.0008 | 0.31 |
| 8.09 | $H_2S$ | –1.27 | –1.79 | 98.31 | –3.68 | –1.52 | –0.43 | 0.47 |
| 7.13 | $C_1$ | –1.21 | –2.04 | –2.069 | 114.84 | –1.50 | –0.43 | 0.55 |
| 7.91 | $C_{2-3}$ | –1.32 | –1.972 | –2.44 | –3.90 | 88.00 | –0.67 | 0.26 |
| 11.12 | $C_{4-6}$ | –2.74 | –3.50 | –4.47 | –6.40 | –3.50 | 69.21 | –0.78 |
| 11.46 | $C_{7-11}$ | –4.06 | –4.72 | –5.99 | –7.84 | –4.93 | –3.36 | 51.25 |
| 46.52 | $C_{12+}$ | | | | | | | |

Table 1—Initial oil compositions ($z_i$ in mol%) for $n_c = 8$ (pseudo)components and effective diffusion coefficients [$\phi D_{ij} \times 10^{-12}$ m$^2$/s (where $i, j = 1, \ldots, n_c - 1$ and $\phi$ is the porosity)].

corresponds to approximately an order-of-magnitude range in volumetric production rates for the different domain sizes that we consider. We also consider the effect of lower production rates.

Before presenting our results, we point out a numerical subtlety: For a rectilinear network of fractures aligned with the coordinate axes, there is no gravitational (flux) component along the direction of perfectly horizontal fractures. This tends to underestimate the (buoyant component of) flow of fluids from horizontal into vertical fractures (and vice versa). To remedy this potential issue, we take advantage of the unstructured grid implementation of our higher-order FE methods for flow and transport, and consider domains with a small dip angle (with a fracture grid that is tilted by 2°).

## Results and Discussion

**Water Coning in 2D 52 × 200 m$^2$ Fractured Cross Section.** In the first set of simulations, we consider a $52 \times 200$ m$^2$ 2D subsection of the reservoir with $4 \times 4$ m$^2$ matrix blocks, surrounded by discrete fractures. The domain is discretized by $27 \times 101$ elements. This relatively small domain size allows us to perform some preliminary parameter-sensitivity studies, before considering larger domains. First, we consider the effect of the distance between the production well and the water–oil contact. We perform four simulations in which a single vertical well is placed on the right boundary (perforated by a fracture) at $z = 32$, 80, 132, and 176 m above the water–oil contact. An additional simulation considers a perforated horizontal well over the full (top) width of the domain.

**Fig. 4** shows grid, the location of the production wells, and the water saturation throughout the domain at $t = 1$ year for the four different depths of vertical wells, and for a horizontal well. We find that breakthrough of water occurs very early—after less than 2 weeks for the lowest well, and up to approximately 1 to 2 months for the vertical and horizontal wells in the top of the reservoir. After a year, water has reached nearly every fracture in the domain below the production well, although at low saturations (<1%).

**Fig. 5** shows the water saturation after producing for 5 years (at 5% HCPV/yr). For all cases, breakthrough of water occurred early, but for wells near the top of the reservoir, the water saturation near the wells is still manageable (<10%). We also observe a

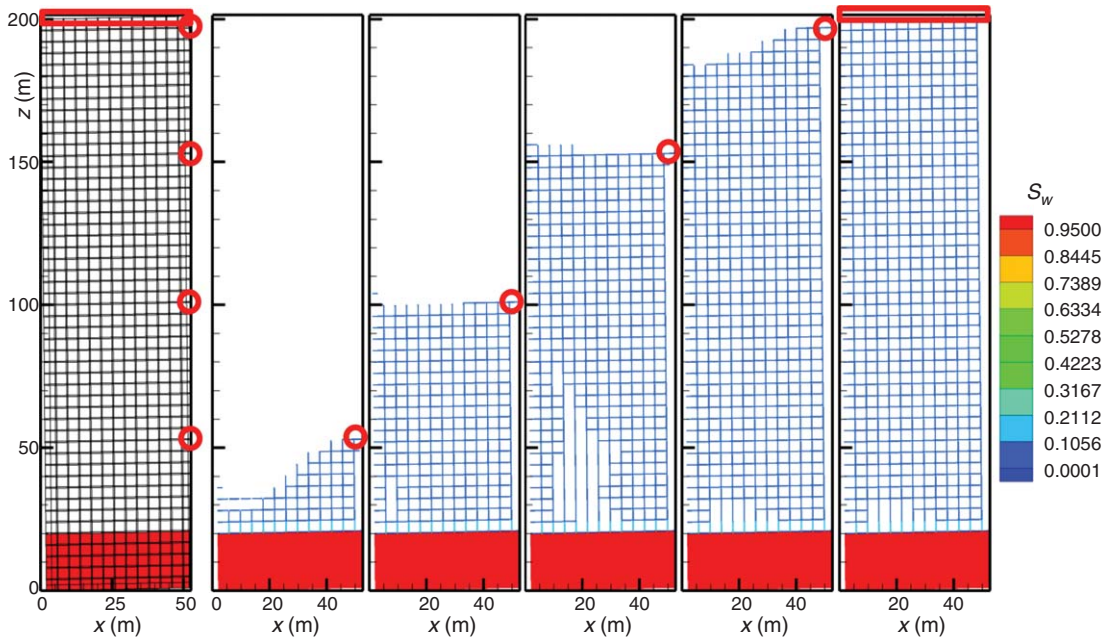


**Fig. 4—27 × 101 element grid for 52 × 200 m$^2$ domain with 4 × 4 m$^2$ matrix blocks and 40-cm CFE elements (left). Red circles indicate the location of vertical production wells for four different simulations, the red rectangle indicates the location of a horizontal well, and the red grid cells represent the aquifer. Water saturations are shown (right five panels) for simulations in which a vertical production well penetrates to a distance *z* from the water–oil contact, for *z* = 32, 80, 132, and 176 m, as indicated by circles. The right-most panel is for a horizontal well spanning the width of the domain. Results are shown at *t* = 6 months.**

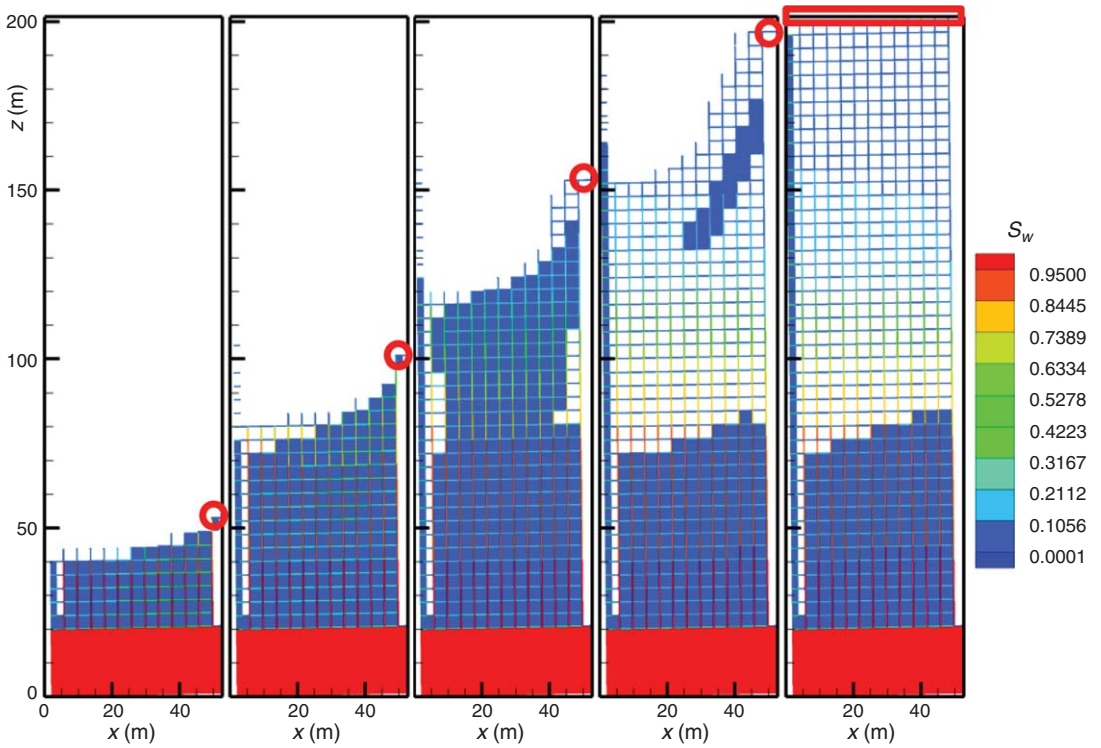


**Fig. 5—Same as Fig. 4 but at $t = 5$ years.**

benefit from the rise of the water level in the bottom of the reservoir, which aids recovery of oil from the matrix blocks through gravity.

Water production and oil recovery for the previous simulations are summarized in **Fig. 6.** We see that some breakthrough of water occurs early in all cases, but that the increase in water saturation after initial breakthrough is quite different depending on the location of the production well. When the well is close to the water–oil contact, water production will increase significantly early on, but when the well is further from the water table (>100 m), the produced water saturation increases only slowly. Interestingly, we find that there is early breakthrough, followed first by a period of near-constant water production and, after approximately 6 years, a second period of steeper increase in water production. This has also been observed in experiments where $n$-$C_5$ was injected in a fractured stack saturated with $n$-$C_{14}$ (Firoozabadi and Markeset 1994).

In terms of oil recovery, remember that the initial fraction of oil in the fractures is 20%, and 33% is in the fractures and the vugs. When the production well is close to the water–oil contact, significant water production occurs early, and oil is mostly recovered from the relatively small area between the aquifer and the well. The oil recovery is less than the amount of oil in the fractures and vugs. On the other hand, if production is from the top, most of the oil in the fractures is eventually recovered.

The general (and obvious) conclusion is that placing the production wells as far away as possible from the aquifer reduces coning. We will therefore focus on either single (vertical) or horizontal wells in the top of the reservoir. From Fig. 6, it may appear as if there is no significant difference in a single vertical well or a horizontal well in the top of the domain. However, this is mostly because of the relatively small width of the domain considered so far. For larger domains, we expect the water level to rise more slowly far away from the producer and the relative coning effect

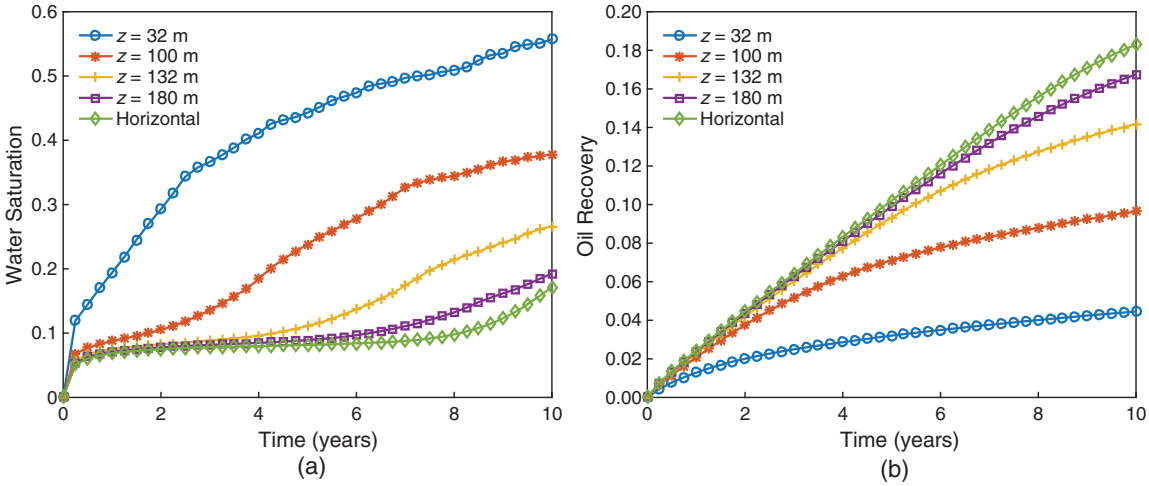


**Fig. 6—Water saturation in the production well (a) and oil recovery (b) for simulations in which a vertical production well penetrates to a distance $z$ from the water–oil contact, for $z = 32$, 80, 132, and 176 m, and for a horizontal well in the top. Domain size is $52 \times 200$ m$^2$.**

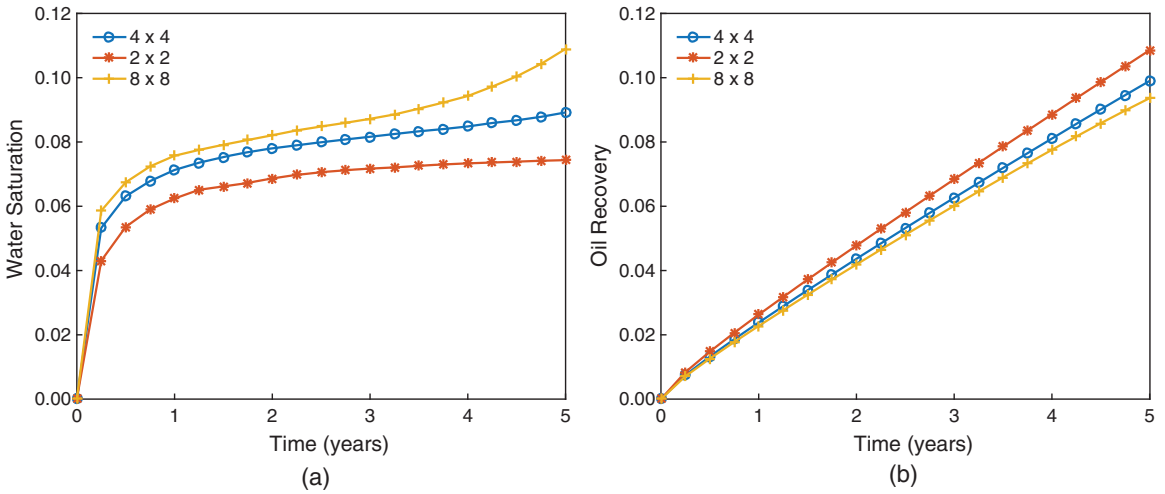


**Fig. 7—Water saturation in the production well (a) and oil recovery (b) for simulations in which the matrix-block size is varied from the base case of $4 \times 4\,m^2$ to $2 \times 2\,m^2$ and $8 \times 8\,m^2$. Domain size is $52 \times 200\,m^2$.**

to be more significant. In that case, using horizontal wells maintains a maximum distance from the aquifer, while distributing the pressure drop over a wider area, thereby reducing the risk of significant coning with early breakthrough.

***Effect of Matrix Block Size on Coning.*** We investigate the effect of matrix-block size (or, equivalently, fracture density) by performing two additional simulations for the same domain size, but with block sizes of $2 \times 2$ and $8 \times 8\,m^2$, respectively. Assuming that oil is recovered mostly from the fractures, we maintained a similar amount of oil in the fractures by halving the fracture aperture in the former case and doubling the aperture in the latter. **Fig. 7** compares the simulated water breakthrough and oil recovery with the $4 \times 4\,m^2$ block base case for 5 years of production. The results are quite similar. The variation is mostly caused by different degrees of vuggyness, because we used the same cross-flow element widths (which represent the vugs) for all cases. As long as the effective permeability of the domain remains equal, a similar amount of oil resides in fractures and vugs, and the fracture network is relatively dense, we expect to see similar degrees of coning.

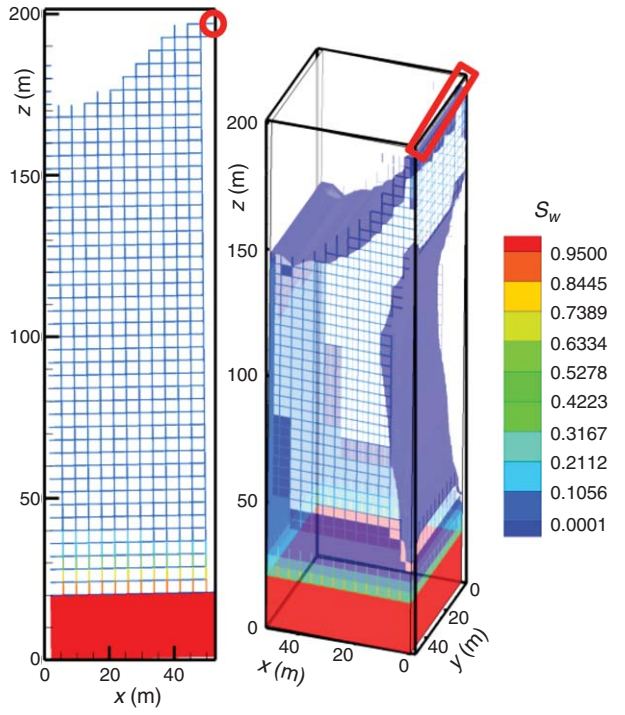


**Fig. 8—Water saturation at $t = 6$ months for 2D and 3D simulations on $52 \times 200\,m^2$ and $52 \times 52 \times 200\,m^3$ domains, respectively.**

***2D vs. 3D Simulations.*** We explore the differences and similarities in 2D vs. 3D simulations for the coning problem by considering a $52 \times 52 \times 200\,m^3$ domain with $4 \times 4 \times 4\,m^3$ matrix blocks and all other parameters as before. Production is at a constant rate of 5% HCPV/yr from a horizontal well along the top $x$-axis ($y = 0$ and $z = 200$ m). The water saturation throughout the domain at $t = 6$ months is shown in **Fig. 8,** as well as for an equivalent 2D simulation. The results are similar, but the coning is slightly less severe in the 3D simulation in which matrix blocks are surrounded by six fractures rather than four in 2D, resulting in a higher fraction of oil in the fractures and vugs. When the fraction of oil in fractures and vugs is kept the same (by reducing the fracture and CFE-element widths in 3D) by symmetry, 2D simulations with a single producing grid cell are equivalent to 3D simulations with a single horizontal well (and a horizontal well in a 2D simulation would correspond to multilateral horizontal wells in 3D simulation). This will be demonstrated further in the numerical examples for $CO_2$ injection. With this understanding, the remaining sensitivity studies will be carried out for 2D grids with a single producing grid cell.

***Effect of Mobility Ratio on Coning.*** Although the oil viscosity of 121 cp is based on a specific fluid and reservoir conditions, we can explore the degree of coning under a broader range of conditions by adjusting the mobility ratio between water and oil. We consider two different scenarios. In the first, we reduce the oil viscosity to 80, 40, and 12 cp (i.e., by up to an order of magnitude) by tuning the critical volume of the residue ($C_{12+}$). In the second, we consider a different wettability in the fractures by reducing the endpoint relative permeability of water in the fractures by an order of magnitude (to 0.1). The latter only reduces the mobility ratio in the fractures, whereas the former also improves gravitational drainage from the matrix blocks. **Fig. 9** shows the water saturation at $t = 5$ years for these four cases, and the breakthrough curves and oil recoveries are presented in **Fig. 10.** We find that a lower water relative permeability in the fractures and a lower oil viscosity of 80 cp only marginally improve the results. However, for oil viscosities of 40 and 12 cp, water breakthrough is delayed by approximately 2 and 5 years, respectively. Oil recovery is more than doubled between the 121- and 12-cp cases. This is not only because of reduced coning, but also because of more efficient drainage from the matrix blocks with a final oil recovery higher than the initial oil in the fractures and vugs.

***Effect of Matrix Wettability and Permeability.*** Next, we consider the effect of rock properties on the degree of coning. We

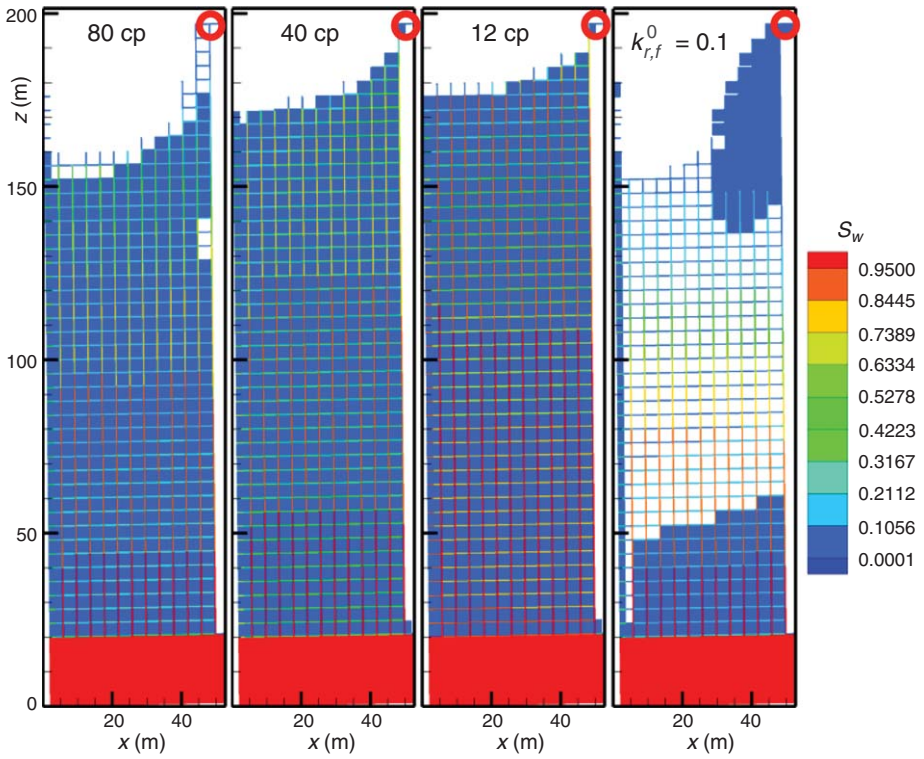


**Fig. 9—Water saturation at $t = 5$ years for simulations in which oil viscosities are reduced from the base case of 121 cp to 80, 40, and 12 cp, as well as a simulation for an endpoint relative permeability of $k^0_{r,f}$=0.1 for water in the fractures. Domain size is $52 \times 200\,m^2$.**

perform a simulation with the same capillary pressure curve as in Fig. 1 for a water-wet rock and three additional simulations (without capillarity) for matrix permeabilities of 10, 100, and 1,000 md. The water saturations at $t = 5$ years are given in **Fig. 11** and the water breakthrough and oil recovery in **Fig. 12.** We find that because of the low oil mobility, capillary imbibition does not significantly affect the results. We also considered a range of different water and oil relative permeabilities in the matrix, but found that this has a negligible impact on the results, because of the low matrix permeability and high oil viscosity.

Increasing the matrix permeability by one or two orders of magnitude is also insufficient to overcome the adverse mobility ratio of a factor ≈500. Only for a matrix permeability of 1,000 md do we see a significant reduction in water production, and associated increase in oil recovery. The final oil recovery for that case is similar to that for a 10 times lower mobility ratio ($\mu_o = 12$ cp) in Fig. 10.

***Effect of Domain Size and Production Rate.*** In the final study of coning, we consider both a domain that is four times wider ($400 \times 200\,m^2$) and one that has a two times thicker oil column ($52 \times 400\,m^2$). The matrix blocks in all cases are $4 \times 4\,m^2$. We also model the effect of production rates with 0.625, 1.25, 2.5, and 5% PV/yr for the wider domain and 2.5 and 5% PV/yr for the taller domain. We find that, for all domain sizes and production rates, water has invaded most of the fractures after a year **(Fig. 13),** although to a lesser extent for lower production rates. **Fig. 14** for the water-production curves and oil recoveries shows that water production is of course reduced for the thicker oil

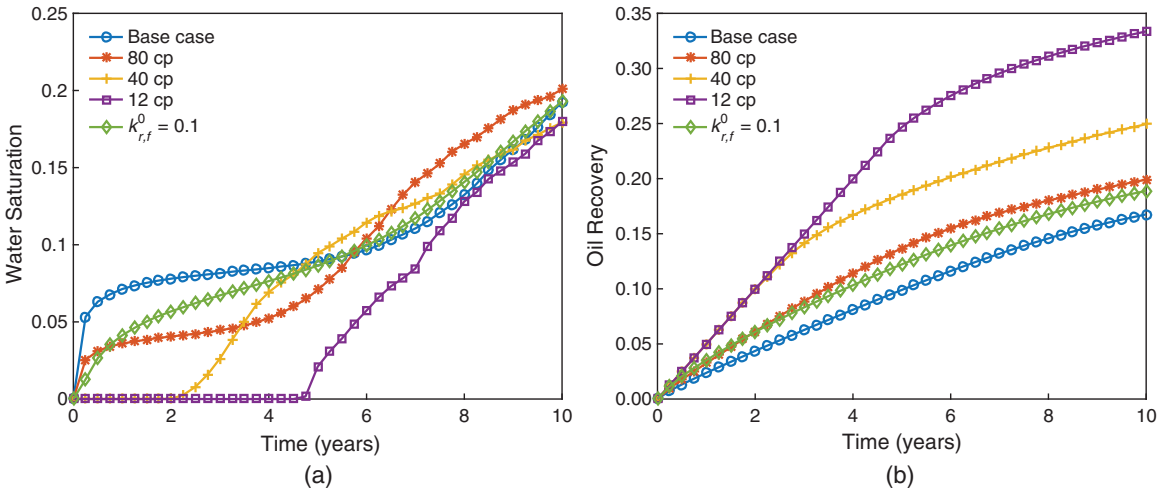


**Fig. 10—Water saturation in the production well (a) and oil recovery (b) for simulations in which oil viscosities are reduced from the base case of $\mu_o = 121$ cp to 80, 40, and 12 cp, as well as a simulation for an endpoint relative permeability of $k^0_{r,f}$=0.1 for water in the fractures.**

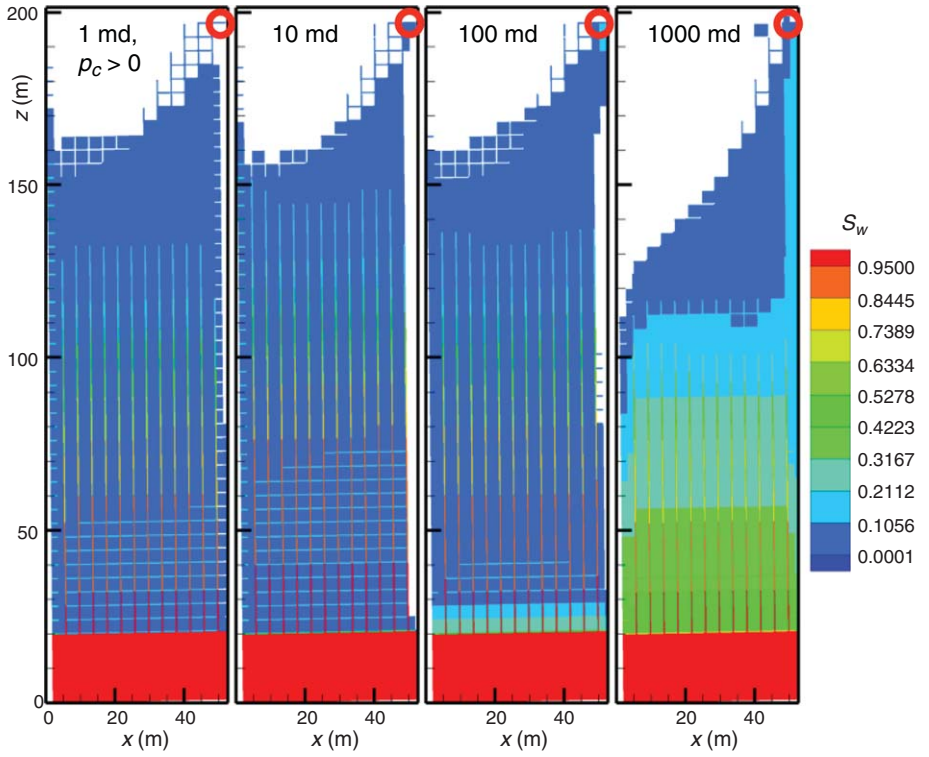


**Fig. 11—Water saturation at $t = 5$ years for a simulation with the capillary pressure from Fig. 1 (left) and for simulations in which the matrix permeability is varied from the base case of 1 md to 10-, 100-, and 1,000-md permeabilities. Domain size is $52 \times 200\ m^2$.**

column (with the production well further above the water aquifer) and for lower production rates, whereas, for the wider domain, the coning is more severe. The degree of coning is reduced for lower production rates, which result in lower pressure gradients (the pressure declines over time are also shown in Fig. 14). We see that, when the rate is halved, the oil recovery is reduced only slightly because of the lower water production. The implication is that, in field applications, the production rate can be reduced to alleviate surface facilities for water separation caused by coning, while maintaining reasonable oil-production performance.

***Effect of Local Viscosity Reduction Around Production Wells.*** One option that has been considered to reduce the coning problem is to spray surfactants or ionic liquids around producing wellbores to reduce the local oil viscosity and associated pressure drop (Subramanian et al. 2015). We have carried out simulations to study whether this approach would indeed mitigate the coning problem. To model a "best-case scenario," we artificially reduced the oil viscosity considerably to 3.6 cp in a 10-m radius around the producing grid cells, and observed the effect that this has on the degree of coning. However, we found that this treatment does not significantly reduce coning or improve oil recovery (results are similar enough that they are not shown in figures). The reason that such a local viscosity reduction does not have a significant impact on coning and oil recovery relates to the pressure profile throughout the domain. Reducing the viscosity in the near-well region only reduces the pressure drop somewhat in that region. The pressure profile throughout the domain is determined by the production rate; the reduction in viscosity and pressure drop near the producer is not "felt" far away at the water–oil contact. Our general conclusion is that reducing the pressure in the near-well

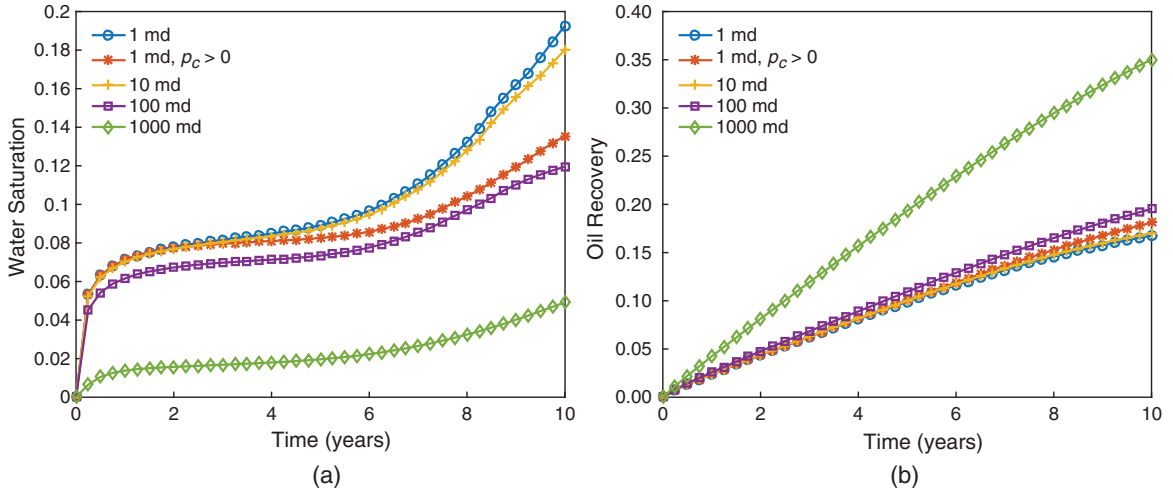


**Fig. 12—Water saturation in the production well (a) and oil recovery (b) for a simulation with the capillary pressure from Fig. 1 (left) and for simulations in which the matrix permeability is varied from the base case of 1 md to larger 10, 100, and 1000 md permeabilities.**

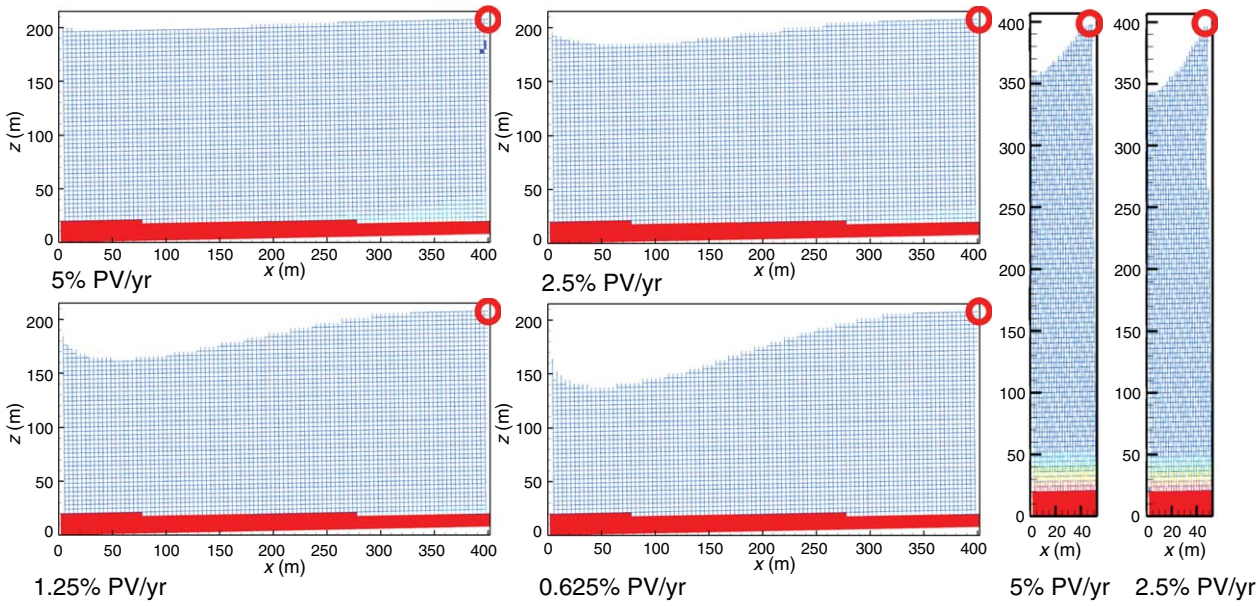


**Fig. 13—Water saturation at $t = 1$ year for simulations in which the domain size is varied from the base case of $52 \times 200\,m^2$ to a much wider domain of $400 \times 200\,m^2$ or a much thicker domain of $52 \times 400\,m^2$. Injection rates of 0.625, 1.25, 2.5, and 5% PV/yr are modeled for the former and rates of 2.5 and 5% PV/yr for the latter.**

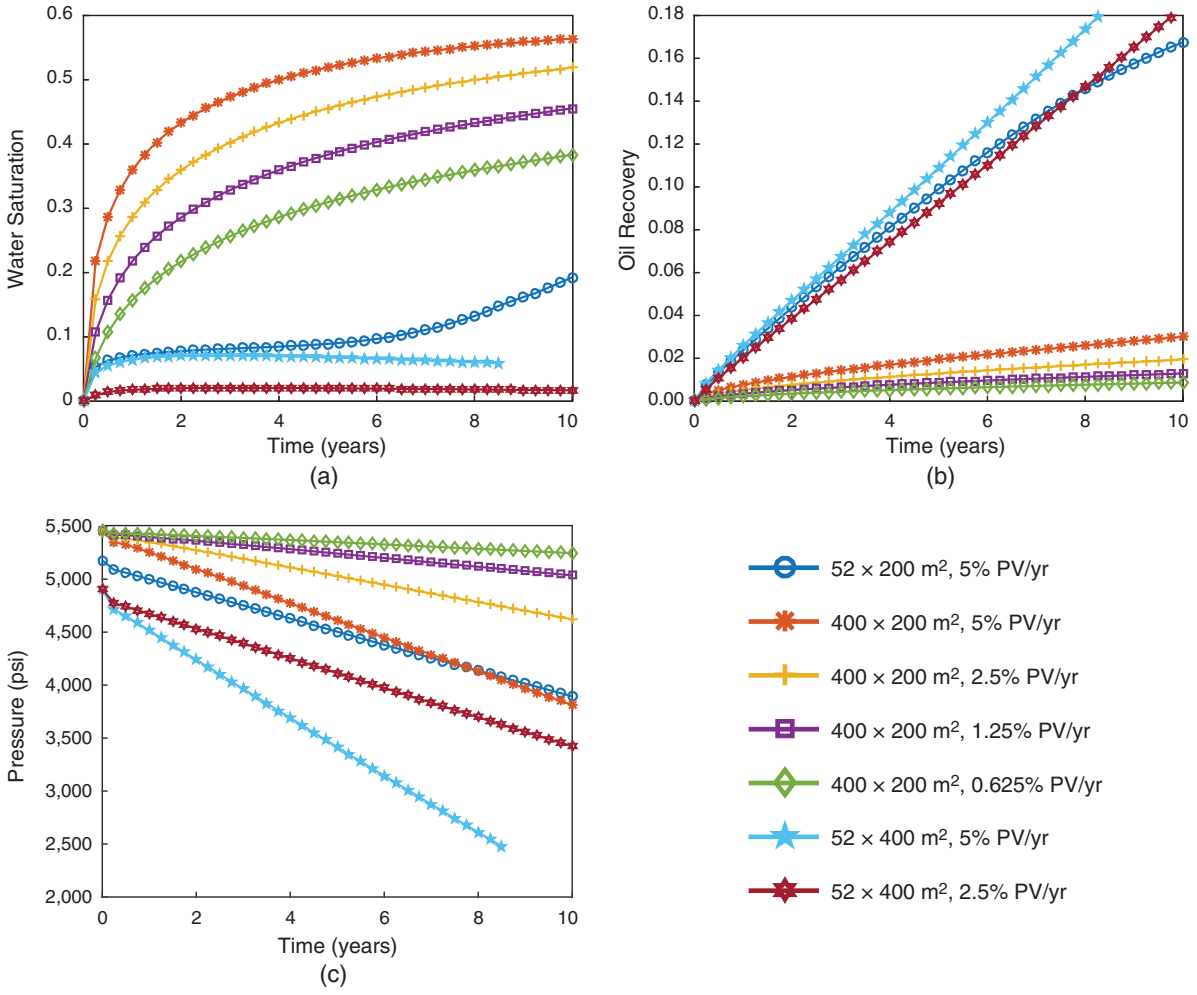


**Fig. 14—Water saturation in the production well (a), oil recovery (b), and pressure in production well (c) for simulations in which the domain size is varied from the base case of $52 \times 200\,m^2$ to a much wider domain of $400 \times 200\,m^2$ or a much thicker domain of $52 \times 400\,m^2$. Injection rates of 0.625, 1.25, 2.5, and 5% PV/yr are modeled for the former and rates of 2.5 and 5% PV/yr for the latter.**

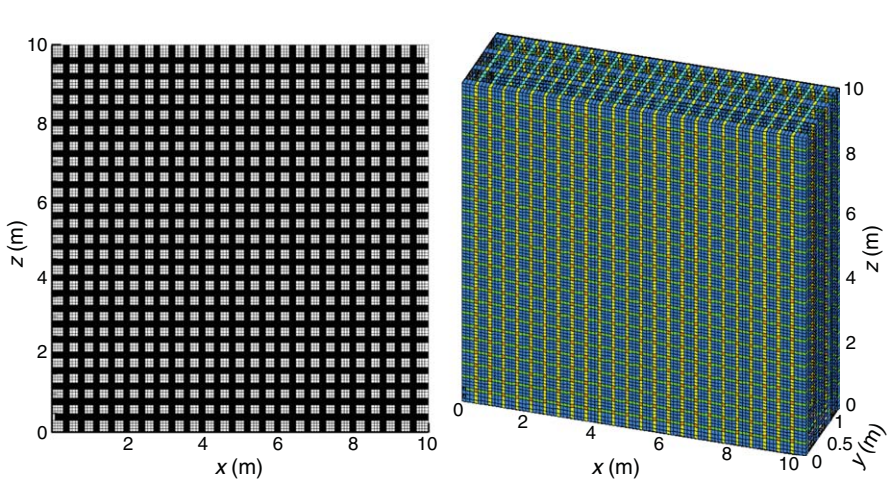


**Fig. 15—99 × 99 element 2D mesh and 99 × 13 × 99 element 3D mesh (Grid 2) and with matrix blocks of 40 cm in each direction surrounded by fractures (and vugs).**

region may improve practical productivity constraints, but does not prevent the coning of water. Instead of reducing the oil viscosity, it is also possible to increase the water viscosity through polymers or gel, but this is impractical for a large underlying aquifer.

***$CO_2$ Injection and Fickian Diffusion.*** Oil recovery from certain densely fractured heavy-oil reservoirs may be enhanced considerably through $CO_2$ injection. When roughly equal volumes are injected and produced, the pressure gradients throughout the reservoirs are much smaller than for production without injection, and water coning is generally less severe, as long as the production wells are sufficiently far above an underlying aquifer. The density difference between $CO_2$ (0.65 $cm^3$/g) and the heavy oil is much larger than for water, which aids gravitational drainage. More importantly, $CO_2$ has a high solubility in this oil (75 mol%), and when it mixes with the oil, it leads to considerable swelling of the oil volume (up to 40%), and, most interestingly, a viscosity reduction to as low as 4 cp. The combination of these favorable phase-behavior effects can significantly improve oil recovery, which we demonstrated in an earlier work through 2D simulations (Moortgat and Firoozabadi 2013a). Here, we extend this problem to a 3D discretely fractured domain to contrast the high efficiency of $CO_2$ injection to the adverse coning issues related to depletion, as discussed previously. We compare 3D simulations to 2D results, perform simulations with and without modeling Fickian diffusion, and compare results to a commercial dual-porosity simulator.

We first consider an optimal scenario in which the matrix blocks are small and the fractures densely spaced, before modeling $CO_2$ injection in the same domain as for the coning study. Specifically, we study a densely fractured domain with $40 \times 40 \times 40\,cm^3$ matrix blocks, surrounded by crossflow elements that represent fractures and connected vugs. To facilitate fine-mesh simulations, we consider a $10 \times 1.2 \times 10\,m^3$ 3D subsection, such that we have three matrix blocks in the $y$-direction and 25 blocks in the $x$- and $z$-direction. We perform simulations on two different grids: Grid 1 ($51 \times 11 \times 51$) and Grid 2 ($99 \times 13 \times 99$) elements, which have ≈90,000 and ≈400,000 degrees of freedom (faces) in our pressure solution. **Fig. 15** shows Grid 2, as well as a $99 \times 99$ element 2D cross section. A subtlety in comparing 3D to 2D simulations, as mentioned for the 3D coning simulations, is that, for a given fracture/CFE width, the fractional PV in the fractures and vugs will be larger in the 3D setup (with fractures surrounding six sides of each matrix cube) than in the 2D case (fractures on four sides of each rectangular matrix block). In most applications, the amount of oil in the fractures is small compared with that in the matrix, and this is not an issue. However, in this particular triple-porosity reservoir, the majority of oil may reside in the fractures and vugs, so we have to be careful in constructing our numerical representation. Specifically, for the 3D case, we consider 1-mm fracture apertures and 10-cm-wide CF elements (accounting for connected vugs), whereas in the 2D simulations, we have 1.5-mm fracture apertures and 17-cm-wide CF elements. With this setup, 9% of the oil resides in the fractures alone whereas 67.5% is contained in the fractures and vugs together (the high end of estimates for this reservoir).

The domain is initially saturated with the same heavy oil as in the coning study and at the same initial temperature and pressure. The $CO_2$ density at reservoir conditions is given previously, and the viscosity is 0.035 cp. We consider an ROS of 50% and quadratic relative permeabilities with endpoint relative permeabilities of 0.4 for both oil and gas. The gas-endpoint relative permeability is low because $CO_2$ is believed to alter the wettability (Müller 2011; Moortgat et al. 2013). This change in wettability can be partly accounted for by endpoint relative permeabilities. Because of the high solubility of $CO_2$ in this oil, and the high reservoir pressure, capillary pressure is negligible in this problem, whereas Fickian diffusion is critical. The full matrix of (composition-dependent) diffusion coefficients for the initial oil is provided in Table 1.

In our simulations, $CO_2$ is injected at a constant rate of 25% PV/yr from the top right (from a horizontal well for the 3D case) with constant-pressure production from the bottom left. **Fig. 16** shows the molar fraction of $CO_2$ throughout the domain at 100% PVI for simulations without and with consideration of Fickian diffusion and for both 2D and 3D simulations. For the latter, we compared a cross section of a fine 3D grid with 2D results. We find that, without diffusion, recovery is mainly from the fractures and vugs with much slower recovery from the matrix blocks through gravitational drainage. For $CO_2$ injection, a dense network of fractures is beneficial, because it offers a large interaction surface between the fractures and the matrix through which species can transfer driven by Fickian diffusion. The $CO_2$ that diffuses into the matrix blocks leads to swelling of the oil, which expels it from the tight matrix, and significantly reduces the oil viscosity, aiding gravitational drainage. The extent of the latter effect is clear from **Fig. 17** which shows the viscosity throughout the domain for simulations with and without diffusion. Without diffusion, the viscosity reduction mostly affects the oil in the fractures and vugs, whereas through diffusion, the viscosity is reduced to less than 10 cp in most of the domain.

The benefits from $CO_2$ injection and the importance of Fickian diffusion are clear from the recovery plots in **Fig. 18a,** which shows results on 2D and both 3D grids and with and without Fickian diffusion. Recovery is high both with and without diffusion, because a large fraction of the oil resides in the fractures and vugs from which it is readily recovered. Diffusion, however, facilitates significant recovery of matrix oil beyond gravitational drainage, which provides 20% incremental recovery. When the fraction of oil in the matrix blocks is higher, Fickan diffusion can more than double the oil recovery, as demonstrated next. Fig. 18 also shows that the 3D results on Grid 1 and Grid 2 have converged, and that

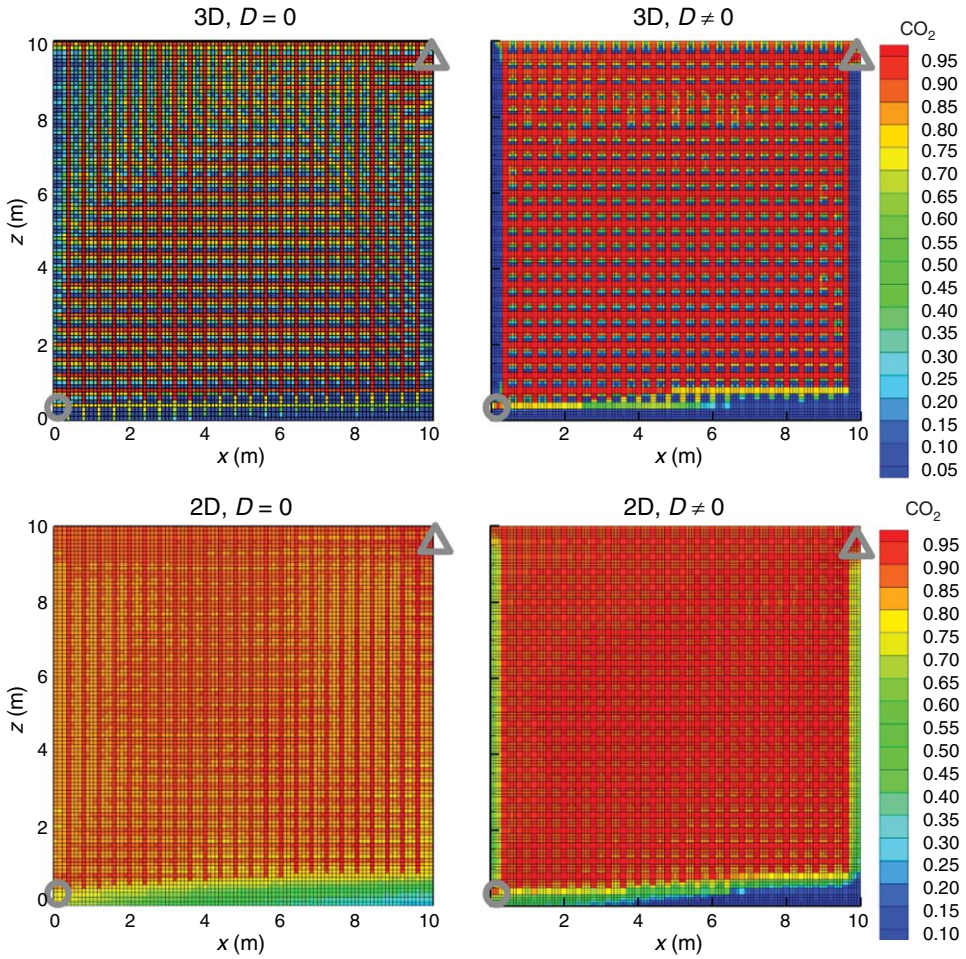


**Fig. 16—$CO_2$ molar fraction for 2D simulations and for a cross section at $y = 0.6$ m of 3D simulations without ($D = 0$) and with ($D \neq 0$) Fickian diffusion. Injection well is indicated by a triangle, production well by a circle.**

simulations on a 2D cross section can accurately predict those from a full 3D simulation. The latter is somewhat unexpected, because in 3D simulation, the surface area between the fractures and matrix is larger than in the 2D representation. The good agreement is most likely caused by the small matrix blocks considered here, which are quickly saturated with $CO_2$. For much larger matrix blocks, the diffusive propagation front of $CO_2$ into the matrix may be more sensitive to the surface area.

To correctly predict oil recovery from $CO_2$ injection in densely fractured reservoirs, one needs a self-consistent model for Fickian diffusion that can account for the diffusive flux between gas in the fractures and single-phase oil in the matrix blocks. Most reservoir simulators rely on a diagonal matrix of constant self-diffusion coefficients and ad hoc approximations to calculate the diffusive flux between neighboring grid cells that are each in a different single phase. However, recently, Halliburton has implemented our

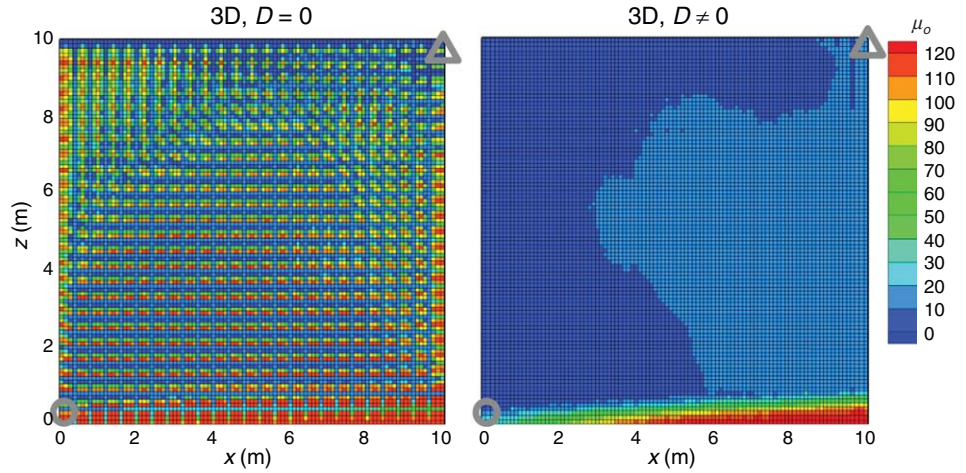


**Fig. 17—Oil viscosity (cp) for a cross section at $y = 0.6$ m of 3D simulations without ($D = 0$) and with ($D \neq 0$) Fickian diffusion. Injection well is indicated by a triangle, production well by a circle.**

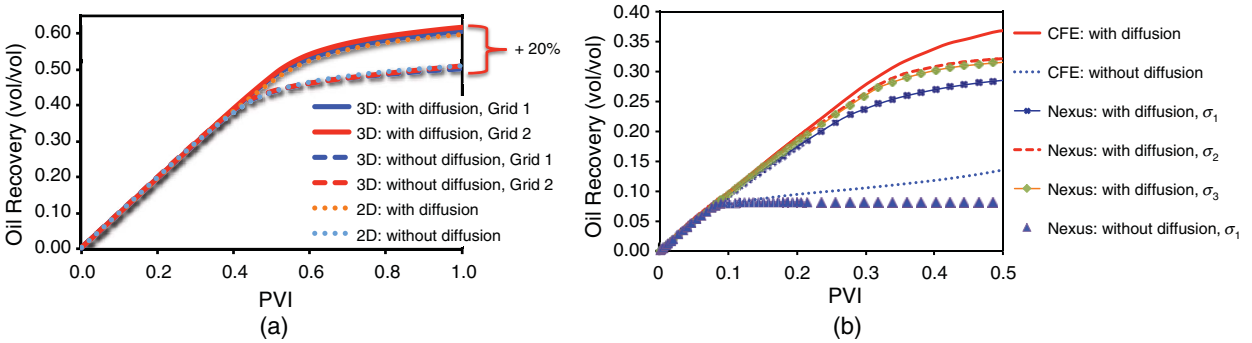


**Fig. 18—Oil recoveries for $CO_2$ injection in 2D and 3D densely fractured domains with and without Fickian diffusion (a) and a comparison between our CFE model and the dual-porosity Nexus reservoir simulator with three different shape factors defined in Eq. 1.**

improved diffusion model into their next-generation Nexus simulator. We used the implicit dual-porosity single-permeability option in Nexus to simulate the example in Moortgat and Firoozabadi (2013a) with 1-mm-wide fractures and 2-cm-wide CFE elements in our discrete-fracture model, such that only 8% of the oil resides in fractures and vugs. The dual-porosity results depend on which shape factor is chosen. We considered three different shape factors, referred to as $\sigma_1$ (Kazemi et al. 1976), $\sigma_2$ (Lim and Aziz 1995), and $\sigma_3$ (Coats 1989), which are given in terms of the effective size of the matrix blocks as

$$\sigma_1 = \frac{4}{L^2}, \quad \sigma_2 = \frac{\pi^2}{L^2}, \quad \sigma_3 = \frac{8}{L^2}, \quad \text{with}$$
$$\frac{1}{L^2} = \left(\frac{1}{L_x^2} + \frac{1}{L_y^2} + \frac{1}{L_z^2}\right) = 18.75\,\text{m}^{-2}. \quad \ldots\ldots\ldots\ldots (1)$$

Fig. 18b compares the oil recoveries with and without diffusion for both simulators. The purely convective dual-porosity results are insensitive to the choice of shape factor, whereas we find that both the Lim and Aziz (1995) and Coats (1989) shape factors provide reasonably similar oil recoveries to our discrete-fracture results with diffusion. The differences may be partly caused by our submatrix block grid resolution, which allows the $CO_2$ front to penetrate the matrix blocks earlier and more effectively, even without diffusion [as can be seen in Figs. 5 and 6 in Moortgat and Firoozabadi (2013a)]. Although we cannot determine the exact source of the discrepancy between our model and Nexus, the difference is already present in the comparison of the purely convection cases. The key point is that the incremental recovery caused by diffusion for the two models is roughly the same.

Two other widely used commercial reservoir simulators were unable to reproduce these results because of the representation of diffusion, fractures, and/or phase behavior.

***$CO_2$ Injection Into Fractured Domain With Underlying Aquifer.*** As a last example, we model $CO_2$ injection in the same base-case $52 \times 200\,\text{m}^2$ domain, as in the coning study, and with the same $4 \times 4\,\text{m}^2$ matrix blocks (e.g., 100X larger). The fracture apertures and all other rock and fluid properties are the same as in that example. $CO_2$ is injected at 2.5% PV/yr from the top-right corner, and production is from the left, 80 m above the water–oil contact, as indicated in **Fig. 19,** which shows the $CO_2$ molar fraction and oil viscosity throughout the domain at 30% PVI for simulations without and with Fickian diffusion. **Fig. 20** shows the corresponding oil recovery and molar fraction of $CO_2$ in the production stream, as well as results for an injection rate of 5% PV/yr. The results are remarkably similar to those for the smaller domain with smaller matrix blocks. Because of diffusion, $CO_2$ is able to fully saturate the matrix blocks, improve the matrix oil

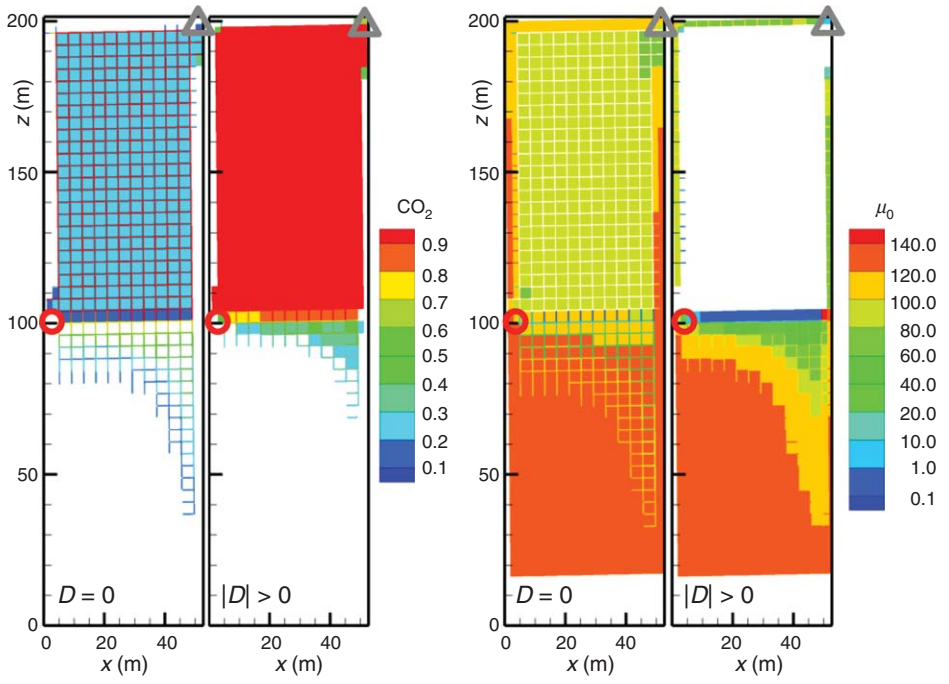


**Fig. 19—$CO_2$ molar fraction (left) and oil viscosity (right) for simulations of $CO_2$ injection at 2.5% PV/yr without and with diffusion on the same grid as in Fig. 4.**

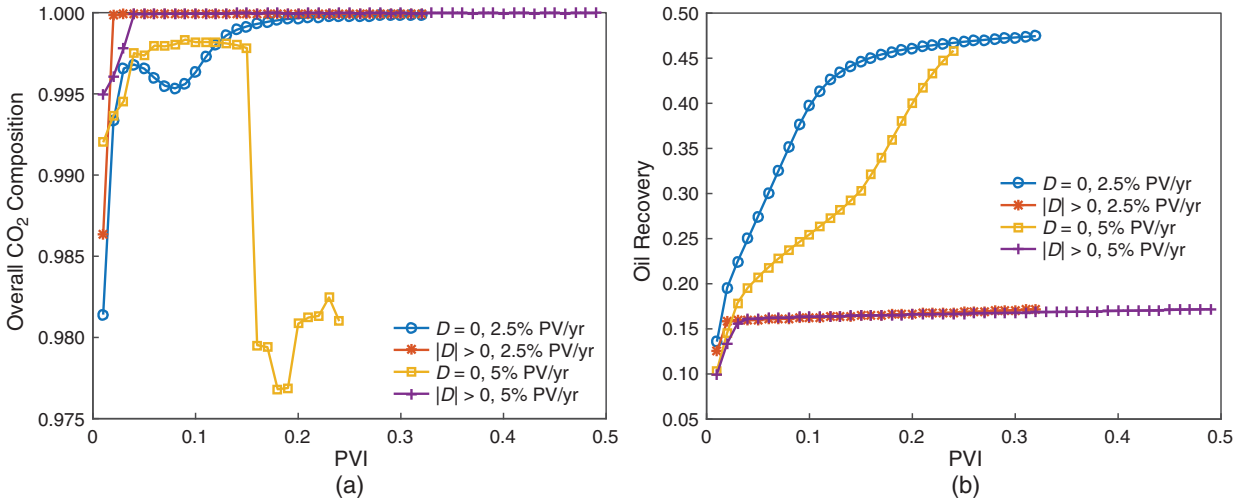


**Fig. 20—$CO_2$ molar fraction in the production well (a) and oil recovery (b) for simulations of $CO_2$ injection without and with diffusion on the same grid as in Fig. 4.**

properties through phase behavior, and increase oil recovery by a factor of three. Without diffusion, the oil recovery as a function of PVI does not show a dependence on the injection rate, whereas the effectiveness of diffusion is greater for lower injection rates, which give diffusion more time to compete with advective flow through the fracture network. These results suggest that, even at the field scale, $CO_2$ injection in fractured reservoirs may be highly beneficial.

We note that the qualitative results from our $CO_2$-injection study apply to a broader pressure range: for pressures from 3,000 to 6,000 psi, the $CO_2$ solubility in this oil varies from 65 to 74 mol%, the initial oil viscosity ranges from 90 to 130 cp, and the fully $CO_2$-saturated oil ranges from 6.4 to 4.7 cp, respectively. In other words, for a wide range of pressures, the $CO_2$ solubility is high, and the viscosity reduction is significant. For much lower temperatures (e.g., at 70° F), the $CO_2$ solubility is still 54 mol%, but both the initial oil viscosity and the fully saturated oil viscosity increase significantly, and even oil production through $CO_2$ injection may prove ineffective.

## Conclusions

In this work, we studied challenges related to the production of heavy viscous oil from fractured and vuggy reservoirs with a strong underlying aquifer. In reservoirs with a tight (low-permeability) matrix rock saturated with viscous oil, gravitational drainage and capillary imbibition of matrix oil during depletion or waterflooding are slow, and oil is mostly recovered from fractures and connected vugs. For such reservoirs to be attractive for hydrocarbon production, a large fraction of the oil should reside in these high-permeability conduits for flow. We consider reservoirs in which 20–50% of the oil is contained in fractures and vugs, which also make up the bulk of the effective permeability of ≈1 darcy (for a fracture permeability of 100 darcies). As a base case, we consider a matrix permeability and (intrinsic) porosity of 1 md and 8%, respectively, an oil viscosity of 121 cp. Because water has a much lower viscosity than the oil, there is an inherent risk of coning when oil is produced from reservoirs with an underlying aquifer.

The numerical investigations in this work were performed with our higher-order FE reservoir simulator, which incorporates a discrete-fracture model that is based on the crossflow equilibrium approach. The performance of our simulator was first demonstrated by modeling a set of experiments in which water was injected at different rates into a stack of chalk blocks separated by a number of discrete fractures. We found excellent agreement between the experimental and simulated results, which show that, at low injection rates, capillary imbibition of water from the fractures into the matrix blocks can be so efficient that the waterfronts in the fractures and the matrix propagate at the same rate, resulting in near piston-like displacement of matrix oil. In earlier work (Moortgat and Firoozabadi 2013b, 2013c), we showed that the same is true at the reservoir scale as long as the matrix blocks are sufficiently small. This numerical experiment highlights the high CPU efficiency of our model compared with a control volume finite-difference method that was used to model this same experiment (Monteagudo and Firoozabadi 2007).

We then studied the risk and degree of coning when oil is produced without injection from a densely fractured heavy-oil reservoir with an underlying aquifer, as well as the potential of $CO_2$ injection as an enhanced-oil-recovery (EOR) strategy.

For the coning study, we carried out an extensive parameter study, investigating the impacts of (1) production well types and placement, (2) domain sizes, (3) oil viscosity, (4) water and oil relative permeabilities in the matrix, (5) relative permeability in the fractures, (6), capillary pressures (wettability), (7) matrix permeability, (8) matrix-block sizes, (9) production rates (or, equivalently, pressure gradients), and (10) a local viscosity reduction around producing wellbores. Our conclusions related to coning can be summarized as follows:

1. For all parameters considered, breakthrough of water occurs early, but the amount of water production at later times depends on rock and fluid properties. The amount of water production may remain manageable for years before increasing again.
2. Coning was not significantly affected by varying the matrix block sizes from $2 \times 2\,m^2$ to $4 \times 4\,m^2$ and $8 \times 8\,m^2$.
3. For low matrix permeabilities, coning and oil recovery are insensitive to water and oil relative permeabilities in the matrix.
4. A reduction of water mobility (only) in the fractures by an order of magnitude only modestly delayed the early breakthrough of water and improved oil recovery by ≈12% incremental.
5. The degree of coning (and resulting poor oil recovery) for 80-cp oil was found to be similar to the 121-cp base case. For 40- and 12-cp oils, breakthrough is delayed by 2 and 5 years, respectively, and oil recovery is 1.5 to 2 times higher.
6. Capillary pressures did not significantly affect the process under the conditions of this study.
7. Increasing the matrix permeability from 1 md to 10 and 100 md only marginally improved the results. For a matrix permeability of 1,000 md, water breakthrough still occurred very early, but water saturations in the production streamed stayed below 2% for approximately 5 years and below 5% for most of the 10 years of production. Oil recovery was approximately twice that of the base case.

8. For a thicker oil column with production wells in the top, coning is obviously reduced.
9. Reducing the oil viscosity around wells (by spraying surfactants or ionic liquids) may improve productivity, but does not significantly reduce coning because it does not affect the pressure gradients at the water–oil contact.
10. High production rates increase the degree of coning. Similar oil recovery can be achieved at reduced production rates, because of the lower amount of water production.
11. Well placement and types: Coning can be reduced by increasing the production-well surface area, placed far above the water–oil contact. Horizontal wells are preferable to vertical ones, and multilateral horizontal wells are an improvement over single wells.

For our investigation of $CO_2$ injection in densely fractured rock, we first presented simulation results for relatively small and densely fractured 2D and 3D domains with small matrix blocks of $0.4 \times 0.4\,m^2$ ($\times 0.4\,m$) with the same rock and fluid parameters as the coning study. This showed that we can obtain the same predictions from 2D simulations as from 3D simulations and demonstrated the convergence of our higher-order schemes on coarse grids. We also compared our results with those of a commercial reservoir simulator that uses our same model for Fickian diffusion. Finally, we verified that the promising results from our small-scale domains carry over to the same domain size as the coning examples with an underlying aquifer and 100 times larger matrix blocks.

The advantages of $CO_2$ injection over depletion or waterflooding from densely fractured reservoirs are:

- Fickian diffusion can drive species exchange between $CO_2$-rich gas in the fractures and oil in the matrix blocks, and diffusion does not depend (directly) on the low matrix permeability.
- The degree of Fickian diffusion depends on the size of the gas–-oil interface. A densely fractured formation is actually beneficial for mass transfer between gas and oil phases.
- $CO_2$ is particularly promising because it often has a high solubility in oil and can lead to favorable phase behavior. For the oil considered in this study, the $CO_2$ solubility is 75 mol%, and dissolution leads to up to 40% volume swelling and an oil-viscosity reduction by a factor 25. This favorable phase behavior is not shared by other injection gases, such as nitrogen, which has been injected in offshore fractured reservoirs.
- $CO_2$ also has a low density at the high reservoir pressure, which improves gravitational drainage of oil from the matrix blocks, compared with waterflooding.
- Because of the combined processes of Fickian diffusion and phase behavior, we find that a significant amount of matrix oil can be recovered, whereas simulations without diffusion show mostly production of the oil in the fractures and vugs.

Whether $CO_2$ injection is a feasible option for EOR depends on availability and cost of a $CO_2$ supply.

## Acknowledgments

We appreciate the help of Saeedeh Mohebbinia and Terry Wong at Halliburton in carrying out the simulations with the Nexus reservoir simulator, and appreciate Halliburton's permission to publish these results.

## References

Abass, H. and Bass, D. 1988. The Critical Production Rate in Water-Coning System. Presented at the Permian Basin Oil and Gas Recovery Conference, Midland, Texas, 10–11 March. SPE-17311-MS. http://dx.doi.org/10.2118/17311-MS.

Beveridge, S., Coats, K., and Alexandre, M. 1970. Numerical Coning Applications. *J Can Pet Technol* **9** (3): 209–215. PETSOC-70-03-07. http://dx.doi.org/10.2118/70-03-07.

Chaney, P., Noble, M., Henson, W. et al. 1956. How to Perforate Your Well to Prevent Water and Gas Coning. *Oil Gas J*. **55:** 108.

Coats, K. 1989. Implicit Compositional Simulation of Single-Porosity and Dual-Porosity Reservoirs. Presented at the 10th SPE Symposium Reservoir Simulation, Houston, 6–8 February. SPE-18427-MS. http://dx.doi.org/10.2118/18427-MS.

Firoozabadi, A. and Thomas, L. 1990. Sixth SPE Comparative Solution Project: Dual-Porosity Simulators. *SPE J*. **42** (6): 710–763. SPE-18741-PA. http://dx.doi.org/10.2118/18741-PA.

Firoozabadi, A. and Markeset, T. 1994. Miscible Displacement in Fractured Porous Media: Part I—Experiments. Presented at the SPE/DOE Ninth Symposium of Improved Oil Recovery, Tulsa, 17–20 April. SPE-27743-MS. http://dx.doi.org/10.2118/27743-MS.

Geiger, S., Matthäi, S., Niessner, J. et al. 2009. Black-Oil Simulations for Three-Components, Three-Phase Flow in Fractured Porous Media. *SPE J*. **14** (2): 338–354. SPE-107485-PA. http://dx.doi.org/10.2118/107485-PA.

Giger, F. M. 1989. Analytic Two-Dimensional Models of Water Cresting Before Breakthrough for Horizontal Wells. *SPE Res Eng* **4** (4): 409–416. SPE-15378-PA. http://dx.doi.org/10.2118/15378-PA.

Hoteit, H. and Firoozabadi, A. 2005. Multicomponent Fluid Flow by Discontinuous Galerkin and Mixed Methods in Unfractured and Fractured Media. *Water Resour. Res.* **41** (11). http://dx.doi.org/10.1029/2005WR004339.

Hoteit, H. and Firoozabadi, A. 2006. Compositional Modeling of Discrete-Fractured Media Without Transfer Functions by the Discontinuous Galerkin and Mixed Methods. *SPE J*. **11** (3): 341–352. SPE-90277-PA. http://dx.doi.org/10.2118/90277-PA.

Hoteit, H. and Firoozabadi, A. 2008. An Efficient Numerical Model for Incompressible Two-Phase Flow in Fractured Media. *Adv. Water Resour.* **31** (6): 891–905. http://dx.doi.org/10.1016/j.advwatres.2008.02.004.

Jiang, Q. and Butler, R. 1998. Experimental and Numerical Modelling of Bottom Water Coning to a Horizontal Well. *J Can Pet Technol* **37** (10): 82–91. PETSOC-98-10-02. http://dx.doi.org/10.2118/98-10-02.

Kazemi, H., Merrill, L., Porterheld, K. et al. 1976. Numerical Simulation of Water-Oil Flow in Naturally Fractured Reservoirs. *SPE J*. **16** (6): 317–326. SPE-5719-PA. http://dx.doi.org/10.2118/5719-PA.

Letkeman, J. and Ridings, R. 1970. A Numerical Coning Model. *SPE J*. **10** (4): 418–424. SPE-2812-PA. http://dx.doi.org/10.2118/2812-PA.

Lim, K. and Aziz, K. 1995. Matrix-Fracture Transfer Shape Factors for Dual-Porosity Simulators. *J. Pet. Sci. Eng.* **13:** 169–178. http://dx.doi.org/10.1016/0920-4105(95)00010-F.

Lohrenz, J., Bray, B. G., and Clark, C. R. 1964. Calculating Viscosities of Reservoir Fluids From Their Compositions. *J Pet Technol* **16** (10): 1171–1176. SPE-915-PA. http://dx.doi.org/10.2118/915-PA.

Monteagudo, J. E. P. and Firoozabadi, A. 2007. Control-Volume Model for Simulation of Water Injection in Fractured Media: Incorporating Matrix Heterogeneity and Reservoir Wettability Effects. *SPE J*. **12** (3): 355–366. SPE-98108-PA. http://dx.doi.org/10.2118/98108-PA.

Moortgat, J. and Firoozabadi, A. 2010. Higher-Order Compositional Modeling With Fickian Diffusion in Unstructured and Anisotropic Media. *Adv. in Water Resour.* **33** (9): 951–968. http://dx.doi.org/10.1016/j.advwatres.2010.04.012.

Moortgat, J., Li, Z., and Firoozabadi, A. 2012. Three-Phase Compositional Modeling of $CO_2$ Injection by Higher-Order Finite Element Methods With CPA Equation of State for Aqueous Phase. *Water Resour. Res.* **48:** W12511. http://dx.doi.org/10.1029/2011WR011736.

Moortgat, J. and Firoozabadi, A. 2013a. Fickian Diffusion in Discrete-Fractured Media From Chemical Potential Gradients and Comparison to Experiment. *Energ. Fuel* **27** (10): 5793–5805. http://dx.doi.org/10.1021/ef401141q.

Moortgat, J. and Firoozabadi, A. 2013b. Higher-Order Compositional Modeling of Three-Phase Flow in 3D Fractured Porous Media Based on Cross-Flow Equilibrium. *J. Comput. Phys.* **250** (0): 425–445. http://dx.doi.org/10.1016/j.jcp.2013.05.009.

Moortgat, J. and Firoozabadi, A. 2013c. Three-Phase Compositional Modeling With Capillarity in Heterogeneous and Fractured Media. *SPE J*. **18** (6): 1150–1168. SPE-159777-PA. http://dx.doi.org/10.2118/159777-PA.

Moortgat, J., Firoozabadi, A., Li, Z. et al. 2013. $CO_2$ Injection in Vertical and Horizontal Cores: Measurements and Numerical Simulation. *SPE J*. **18** (2): 331–344. SPE-135563-PA. http://dx.doi.org/10.2118/135563-PA.

Müller, N. 2011. Supercritical $CO_2$-Brine Relative Permeability Experiments in Reservoir Rocks—Literature Review and Recommendations. *Transport Porous Media* **87** (2): 367–383. http://dx.doi.org/10.1007/s11242-010-9689-2.

Muskat, M. and Wyckoff, R. 1935. An Approximate Theory of Water Coning in Oil Production. *Trans., AIME* **114:** 144–161. SPE-935144-G. http://dx.doi.org/10.2118/935144-G.

Pérez-Martínez, E., Rodríguez de la Garza, F., and Samaniego-Verduzco, F. 2012. Water Coning in Naturally Fractured Carbonate Heavy Oil Reservoir—A Simulation Study. Presented at the SPE Latin America and Caribbean Petroleum Engineering Conference, Mexico City, Mexico, 16–18 April. SPE-152545-MS. http://dx.doi.org/10.2118/152545-MS.

Pooladi-Darvish, M. and Firoozabadi, A. 2000. Experiments and Modeling of Water Injection in Water-Wet Fractured Porous Media. *J Can Pet Technol* **39** (3): 31–42. SPE-00-03-02-PA. http://dx.doi.org/10.2118/00-03-02-PA.

Saffman, P. G. and Taylor, G. 1958. The Penetration of a Fluid Into a Porous Medium or Hele-Shaw Cell Containing a More Viscous Liquid. *Pro. Roy. Soc. A* **245:** 312–329. http://dx.doi.org/10.1098/rspa.1958.0085.

Schols, R. 1972. An Empirical Formula for the Critical Oil Production Rate. *Erdoel Erdgas, Z.* **88** (1).

Settari, A. and Aziz, K. 1974. A Computer Model for Two-Phase Coning Simulation. *SPE J.* **14** (3): 221–236. SPE-4285-PA. http://dx.doi.org/10.2118/4285-PA.

Singhal, A. 1996. Water and Gas Coning/Cresting—A Technology Overview. *J Can Pet Technol* **35** (4): 56–62. SPE-96-04-06-PA. http://dx.doi.org/10.2118/96-04-06-PA.

Subramanian, D., Wu, K., and Firoozabadi, A. 2015. Ionic Liquids as Viscosity Modifiers for Heavy and Extra-Heavy Crude Oils. *Fuel* **143:** 519–526. http://dx.doi.org/10.1016/j.fuel.2014.11.051.

Tan, C. and Homsy, G. 1986. Stability of Miscible Displacements in Porous Media: Rectilinear Flow. *Phys Fluids* **29** (11): 3549–3556. http://dx.doi.org/10.1063/1.865832.

Verga, F., Viberti, D., and Di Renzo, D. 2005. Are Multilateral Wells Really Effective To Control Water Coning? Presented at the SPE Offshore Mediterranean Conference and Exhibition, Ravenna, Italy, 16–18 March. OMC-2005-055.

Warren, J. and Root, P. 1963. The Behavior of Naturally Fractured Reservoirs. *SPE J.* **3** (3): 245–255. SPE-426-PA. http://dx.doi.org/10.2118/426-PA.

**Joachim Moortgat** is an assistant professor in the School of Earth Sciences, Ohio State University. His research interests are in the theory and advanced numerical modeling of compositional multiphase flow in subsurface fractured porous media. Moortgat holds MS degrees in theoretical physics and astrophysics, both from Utrecht University, The Netherlands, and a PhD degree in astrophysics from the Radboud University, The Netherlands. Moortgat was the recipient of the 2014 SPE Cedric K. Ferguson Medal.

**Abbas Firoozabadi** is the director of the Reservoir Engineering Research Institute in Palo Alto, California, and a faculty member at Yale University in New Haven, Connecticut. He was a Distinguished Visiting Professor at Rice University in the spring semester of 2016. Firoozabadi main research interests are in higher-order reservoir simulation of complex subsurface formations in relation to fluid injection and $CO_2$, sequestration, and molecular structure in bulk phase and in fluid–fluid and fluid–-solid interfaces in relation to oil and gas production and flow assurance. He is the author of a recent book *Thermodynamics and Applications in Hydrocarbon Energy Production*. Firoozabadi has published some 210 journal papers. His honors and awards include the SPE/AIME Anthony Lucas Gold Medal and membership in the US National Academy of Engineering. He holds a BS degree from the Abadan Institute of Technology, Iran, and MS and PhD degrees from the Illinois Institute of Technology, Chicago, Illinois; and he conducted post-doctoral degree research at the University of Michigan, Ann Arbor.